ARTICLE

Structure, Electrical and Oxygen Transport Properties of Fe-Doped $SrCoO_{3-\delta}$ Perovskites

Jian-xin Yi[a*], Shao-jie Feng[b], Qing Zeng[c], Chu-sheng Chen[c]

a. State Key Laboratory of Fire Science, Department of Safety Science and Engineering, University of Science and Technology of China, Hefei 230026, China
b. School of Materials Science and Chemical Engineering, Anhui University of Architecture, Hefei 230022, China
c. CAS Key Laboratory of Materials for Energy Conversion, Department of Materials Science and Engineering, University of Science and Technology of China, Hefei 230026, China

(Dated: Received on November 6, 2014; Accepted on November 18, 2014)

The structure-property relationship of Fe-doped $SrCoO_{3-\delta}$ was studied. With increase of Fe content in $SrCo_{1-x}Fe_xO_{3-\delta}$ from x=0 to x=0.2, the phase composition changed progressively in the order of hexagonal→brownmillerite (main)+hexagonal→cubic (main)+ brownmillerite→single cubic phase. Transition between the hexagonal/brownmillerite phase and the cubic phase took place with variation of the operating conditions, and was associated with remarkable changes in the electrical conductivity and oxygen permeation flux.

Key words: Perovskite, Ceramic membrane, Electrical, Oxygen transport, Structure

I. INTRODUCTION

Perovskite oxides hold great promise as candidate materials for the cathode of solid oxide fuel cells and for oxygen separation membranes [1–5]. For these applications, both high oxide ion conductivity and high electronic conductivity, which strongly correlate with the structure of the materials, are essential. The oxide ion conductivity is significantly governed by the amount and mobility of the oxygen vacancies and extent of lattice distortion, whilst the electronic conductivity depends greatly on the covalent overlapping of B3d and O2p orbitals [4]. Note that the B-O orbital overlapping also symbolizes the extent of lattice distortion. Perovskite oxides of undistorted cubic structure with maximum B−O orbital overlapping usually exhibit high mixed ionic-electronic conductivity.

$SrCoO_{3-\delta}$ (referred to as SCO hereafter) has been widely studied as a model material due to the excellent mixed conductivity at high temperatures [1, 2, 6–9]. At temperatures below ∼900 °C, SCO may transform from cubic perovskite to a hexagonal or brownmillerite phase, leading to significant decrease of the mixed conductivity [2, 6]. One possible way to suppress the detrimental phase transition in SCO is proper substitution of Co. For example, Fe substitution for Co in SCO can effectively stabilize the cubic perovskite structure down to room temperature [4, 8]. Insight into this stabilization process will definitely benefit further materials development. In the present work, we focus on the structural evolution and resulting changes of electrical and oxygen transport properties of SCO due to Fe doping, in order to gain deeper understanding of the structure-property relationship of mixed-conducting perovskites.

II. EXPERIMENTS

$SrCo_{1-x}Fe_xO_{3-\delta}$ (x=0−0.2) powders were prepared via a standard ceramic method. Raw materials of $SrCO_3$ (AR), Fe_2O_3 (AR), and Co_2O_3 (AR) were thoroughly mixed and milled. Calcination of the powder mixture was conducted at 950, 1050, and 1100 °C in ambient air for 10 h each with intermittent grinding. Sintering was performed at 1150 °C for 10 h to obtain ceramic samples.

Phase composition of the materials was examined with X-ray diffraction (XRD, Rigaku D/Max-rA, CuKα). Differential thermal analysis (DTA, Shimadzu DTG-60H) was performed in flowing air stream at a heating rate of 10 °C/min. The electrical conductivity of bar-shaped samples with typical dimension of 25 mm×4 mm×1.5 mm was measured via a four probe method on a ZL5 LCR analyzer. For oxygen permeation measurements, disk-shaped sample with thickness of 1.2−1.3 mm was placed on an alumina tube spaced by a glass ring sealant, and heated to 1000 °C. When the glass ring was softened, the membrane sample was jointed to the alumina tube to form a permeate compartment, and the temperature was subsequently adjusted for permeation measurements. A flowing air stream was fed to one (feed) side and helium to the other (sweep) side of the membrane. The oxygen concentra-

*Author to whom correspondence should be addressed. E-mail: yjx@ustc.edu.cn, Tel./FAX: +86-551-63607817

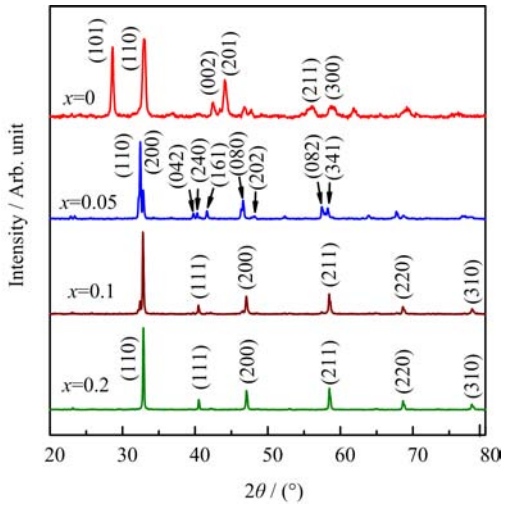

FIG. 1 XRD patterns for as-prepared $SrCo_{1-x}Fe_xO_{3-\delta}$ powders.

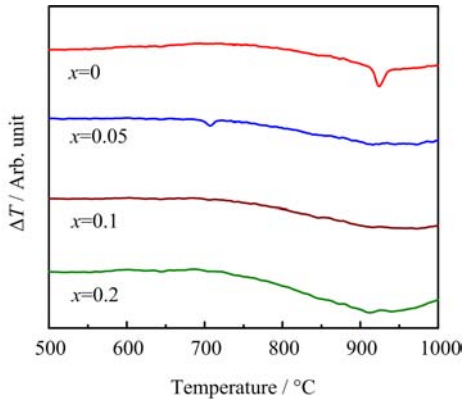

FIG. 2 DTA curves for $SrCo_{1-x}Fe_xO_{3-\delta}$ obtained at a heating rate of 10 °C/min in air.

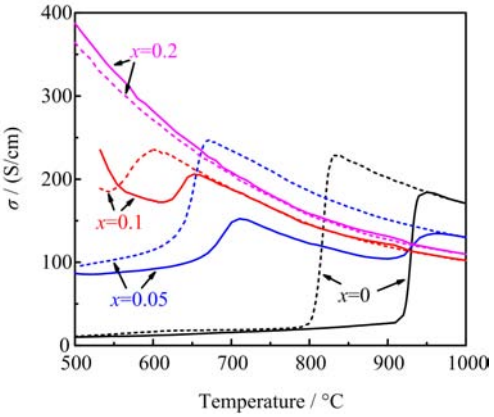

FIG. 3 Electrical conductivity of $SrCo_{1-x}Fe_xO_{3-\delta}$ measured at a heating/cooling rate of 1 °C/min. Solid lines: heating cycle, dashed lines: cooling cycle.

tion in the permeate exhaust was determined with an online GC 9750 gas chromatograph. The oxygen due to leakage through the sealant or membrane, typically less than 5% of the total amount of oxygen in the exhaust, was corrected by measuring the nitrogen concentration.

III. RESULTS AND DISCUSSION

As shown in Fig.1, the XRD pattern of x=0 sample agrees with that of hexagonal $SrCoO_{2.5}$ (JCPDS 48-0875) phase (referred to as H phase). For the x=0.05 sample, a brownmillerite phase (Br phase) close to orthorhombic $Sr_2Co_2O_5$ (JCPDS 34-1475) was observed. When the Fe content was increased to 0.1, the sample consisted of mainly cubic perovskite phase (C phase, JCPDS 82-2445) as well as some minor Br phase. With further increasing the Fe content to 0.2, a single cubic phase was obtained.

Evolution of the phase structure with temperature for the as-prepared samples was studied with DTA (Fig.2). For the x=0 sample, a strong endothermic peak was present at ∼924 °C during heating, corresponding to the H→C phase transition. A similar peak was also observed for x=0.05 sample at temperature of ∼707 °C, which can be ascribed to the Br→C phase transition. The much lower temperature for the Br→C than the H→C phase transition indicated that the former transition required less energy than the latter. As the Fe content increased to 0.1 or above, no distinct peak was observed within the detection limit of the technique. Note that the Br→C transition was not observed for the x=0.1 sample, most likely because only minor Br phase was contained in the sample as revealed by XRD.

The effects of Fe-doping on the electrical conductivity was also investigated at 500−1000 °C (Fig.3). For x=0 sample, the electrical conductivity increased with temperature, and exhibited a drastic jump from 27 S/cm to 187 S/cm at 910−950 °C due to the H→C transition. The reverse jump due to the C→H transition occurred upon cooling at a temperature of 100 °C lower. This hysteresis is characteristic of the first-order H→C phase transition for $SrCoO_{3-\delta}$. For the x=0.05 sample, two conductivity jumps at 650−710 and ∼910−950 °C, corresponding to the Br→C and H→C transition, respectively, were observed upon heating. The H→C conductivity jump suggested presence of trace amount of H phase in the x=0.05 sample which was not detected by XRD and DTA. In contrast, only one conductivity jump, which can be assigned to the C→Br transition, was observed at 670−610 °C during cooling, whereas the expected conductivity drop due to C→H transition was absent. This observation indicated that formation of the H phase was not favorable under the given experimental conditions. Note that the phase composition in $SrCoO_{3-\delta}$ is significantly affected by a few factors like thermal history and oxygen partial pressure [10]. With respect to the x=0.1 sample, only a small conductivity jump at 610−660 °C during heating (Br→C) and at

DOI:10.1063/1674-0068/28/cjcp1411192

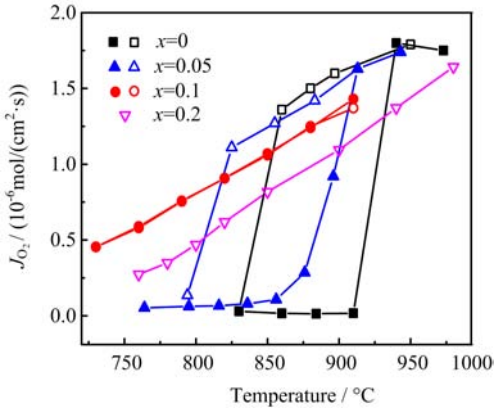

FIG. 4 Oxygen permeation flux J_{O_2} of $SrCo_{1-x}Fe_xO_{3-\delta}$ as a function of temperature. Solid symbols: heating cycle, open symbols: cooling cycle.

540−600 °C during cooling (C→Br) was observed, in line with its phase composition (C and minor Br phase). With further increasing x to 0.2, no conductivity jump was observed.

It can also be seen from Fig.3 that, at higher temperatures (>950 °C) all the samples of different Fe content exhibited cubic structure, the conductivity generally decreased with increasing x, consistent with previous report that Fe substitution for Co reduced the conductivity for perovskites [11]. Contrarily, the reverse trend was observed at lower temperatures where the C phase transformed into the Br or H phase. These results, in combination with the observed conductivity jumps due to the Br→C and H→C transition, reveal that the conductivity follows the order of C>Br>H. For the different phases (C, Br, H) of Fe-doped SCO perovskite, the B−O−B bond angle were determined by previous neutron diffraction studies to be 180°, 129°−174°, and ∼80°, respectively [9, 12]. This indicates decreasing B−O orbital overlapping and increasing lattice distortion in the perovskite, which agrees well with the observed conductivity order (C>Br>H). The small B−O−B angle (*i.e.*, large lattice distortion) for the H phase also accords with the DTA results indicating that the H→C phase transition required more energy than the Br→C transition.

Similar to the conductivity measurement, abrupt changes in the oxygen permeation flux were also observed upon heating for the x=0 and x=0.05 samples (Fig.4). For the former sample, the oxygen flux was almost negligible at lower temperatures, and increased during heating from 1.7×10^{-8} mol/(cm^2·s) at 910 °C to 1.8×10^{-6} mol/(cm^2·s) at 940 °C by two orders of magnitude due to the H→C transition. The reverse flux reduction (C→H transition) took place as the temperature was lowered down to below 860 °C. For x=0.05 sample, the temperature for the jumps of the oxygen flux (H→C or C→H transition) decreased by ∼40 °C, indicating extension of the stability regime for the C phase towards lower temperature. The observed C→H transition in the permeation measurement during cooling for x=0.05, which was absent in the conductivity measurement, may again be due to that the phase composition of SCO varies with the operating conditions as mentioned above [10]. Note that not only the thermal history but also the atmosphere was different in these measurements. During the permeation measurement, one side of the sample was exposed to air and the other side was exposed to helium (*i.e.*, a gradient of oxygen partial pressure), while the sample was exposed to air atmosphere only (without gradient) in the conductivity measurements. For the samples of higher Fe doping level, no abrupt change in the oxygen flux was observed. Nevertheless, the Arrhenius plots of the oxygen permeation flux for the x=0.1 and x=0.2 samples still showed a curvature at around ∼800−820 °C, indicating partial transition of the C phase to the Br phase below this temperature under the oxygen permeation conditions [6]. The much lower oxygen permeation flux of the H and Br phase, resulting from immobilization of the oxygen vacancies due to the lattice distortion [4, 8], highlights the importance of stabilization of the C phase to the oxygen transport property in SCO. It should also be noted that at higher temperatures, similar to the conductivity, the oxygen flux for the C phases decreased with Fe doping, which can be ascribed to reduction in the oxygen nonstoichiometry and oxide ion mobility due to Fe substitution for Co [13].

IV. CONCLUSION

The structure of $SrCo_{1-x}Fe_xO_{3-\delta}$ varied significantly with the Fe content. The phase composition underwent a progressive change of H→(Br, H)→(C, Br)→C with Fe content increasing from 0 to 0.2, leading to significant change in both the electrical and oxygen transport properties. Lower electrical conductivity and oxygen flux were observed for the Br and H phase, which can be attributed to the decreased B−O orbital overlapping and increased lattice distortion.

V. ACKNOWLEDGMENTS

This work was supported by the National Natural Science Foundation of China (No.21076205, No.50972138, and No.U1432108), the Anhui Provincial Natural Science Foundation (1408085ME85), the Fundamental Research Funds for the Central Universities (USTC: WK2320000021), and the Scientific Research Foundation for the Returned Overseas Chinese Scholars, State Education Ministry of USTC (No.WF2320000005).

DOI:10.1063/1674-0068/28/cjcp1411192

[1] A. Aguadero, D. Perez-Coll, J. A. Alonso, S. J. Skinner, and J. Kilner, Chem. Mater. **24**, 2655 (2012).
[2] V. Cascos, R. Martinez-Coronado, and J. A. Alonso, Int. J. Hydrogen Energy **39**, 14349 (2014).
[3] T. Nagai and W. Ito, Solid State Ionics **262**, 650 (2014).
[4] H. J. M. Bouwmeester and A. J. Burggraaf, *CRC Handbook of Solid State Electrochemistry*, Boca Raton: CRC Press, 481 (1997).
[5] J. X. Yi, M. Schroeder, and M. Martin, Chem. Mater. **25**, 815 (2013).
[6] Z. Q. Deng, W. S. Yang, W. Liu, and C. S. Chen, J. Solid State Chem. **179**, 362 (2006).
[7] C. de la Calle, A. Aguadero, J. A. Alonso, and M. T. Fernández-Díaz, Solid State Sci. **10**, 1924 (2008).
[8] T. Nagai, W. Ito, and T. Sakon, Solid State Ionics **177**, 3433 (2007).
[9] W. T. A. Harrison, S. L. Hegwood, and A. J. Jacobson, J. Chem. Soc. Chem. Comm. 1953 (1995).
[10] Y. Takeda, R. Kanno, T. Takada, O. Yamamoto, M. Takano, and Y. Bando, Z. Anorg. Allg. Chem. **540/541**, 259 (1986).
[11] L. W. Tai, M. M. Nasrallah, H. U. Anderson, D. M. Sparlin, and S. R. Sehlin, Solid State Ionics **76**, 259 (1995).
[12] W. T. A. Harrison, T. H. Lee, Y. L. Yang, D. P. Scarfe, L. M. Liu, and A. J. Jacobson, Mater. Res. Bull. **30**, 621 (1995).
[13] J. X. Yi, J. Brendt, M. Schroeder, and M. Martin, J. Membrane Sci. **387**, 17 (2012).

DOI:10.1063/1674-0068/28/cjcp1411192